SPECIAL PROJECT PROGRESS REPORT

Reporting year	2022
Project Title:	Using stochastic surrogate methods for advancing towards reliable meteotsunami early warning systems
Computer Project Account:	SPCRVILI
Principal Investigator(s):	Ivica Vilibić
Affiliation:	Ruđer Bošković Institute (RBI)
Name of ECMWF scientist(s) collaborating to the project (if applicable)	Clea Denamiel, Iva Tojčić (Ruđer Bošković Institute, RBI), Petra Pranić, Petra Zemunik (Institute of Oceanography and Fisheries, IOF)
Start date of the project:	01/01/2021
Expected end date:	31/12/2023

Computer resources allocated/used for the current year and the previous one (if applicable)

		Previous year		Current year	
		Allocated	Used	Allocated	Used
High Performance Computing Facility	(units)	20,000,000	20,000,000	15,000,000	
Data storage capacity	(Gbytes)	30,000	30,000	50,000	

Summary of project objectives (10 lines max)

Due to impossibility to properly reproduce processes at the mesoscale (~1 km), early warning systems for meteotsunamis – atmospherically-induced long ocean waves in the tsunami frequency band – are still far from providing reliable hazard forecasts. This is particularly relevant when the realisation is coming from deterministic atmospheric and ocean models. The aim of this special project is to improve the reliability of the meteotsunami early warning systems, through improving of stochastic surrogate model by extending the pseudo-spectral approximation methodology, and by extensive testing of the model of the documented meteotsunami events. With the latter, more robust results will enlighten if the surrogate methodology may be used for better prediction of meteotsunamis.

Summary of problems encountered (10 lines max)

No major problem was encountered in terms of usage of the supercomputing facilities.

Summary of plans for the continuation of the project (10 lines max)

The project will continue in several ways: (1) by testing the polynomial chaos expansion methodology on higher level (delayed Gauss–Patterson levels 7, 8, 9, 10) and to see if any improvement in reproduction of meteotsunami stochastic forecast is reached, (2) by further quantifying meteotsunami changes in the future climate by using coupled (sub-)kilometre-scale atmosphere-ocean models, for different scenarios and various meteotsunami sites, and (3) by quantifying planetary hazard of meteotsunamis generated by past and potential volcanic explosions coming from super-volcano sites in the world, through coupling of global atmospheric and ocean numerical models..

List of publications/reports from the project with complete references

- Denamiel, C., Tojčić, I., Vilibić, I., 2022. Meteotsunamis in orography-free, flat bathymetry and warming climate conditions. Journal of Geophysical Research Oceans, 127, e2021JC017386. https://doi.org/10.1029/2021JC017386
- Denamiel, C., Vasylkevych, S., Žagar, N., Zemunik, P., Vilibić, I., 2022. Destructive potential of planetary meteotsunami waves beyond the Hunga volcano eruption (Tonga). Earth and Space Science Open Archive [preprint]. https://doi.org/10.1002/essoar.10511565.1

Summary of results

The research done in the last year was directed a bit from the planned activities, as (1) an opportunity emerged to study future climate of meteotsunamis, not done in any parts of the world by using high-resolution atmosphere-ocean models, and (2) explosive eruption of the Hunga volcano in January 2022 and the generated planetary atmospheric waves (Lamb waves) that caused planetary meteotsunami waves, last time observed in 1883 after the Krakatoa explosion, allowed – for the first time – quantification of that hazard by using global atmosphere-ocean models (in addition to observations).

1. Assessing meteotsunami hazard in the future climate

In the meteotsunami community, the Adriatic basin is historically one of the most studied areas in the world due to the 21 June 1978 event when large meteotsunami waves (6 m height for periods of about 20 min) occurred in the port of Vela Luka causing substantial damages to the infrastructures (Fig. 1; Vučetić et al., 2009; Orlić et al., 2010). For this region, most of meteotsunamigenic disturbances are known to develop under similar synoptic conditions (Vilibić and Šepić, 2009; Tojčić et al., 2021) and to propagate from the Apennines to the Croatian coasts (Fig. 1) with associated meteotsunami waves travelling across the Adriatic Sea (Vilibić and Šepić, 2009; Denamiel et al., 2020). However, within the Adriatic Sea meteotsunami community, questions are still raised about (1) the influence of orography on the generation and propagation of the atmospheric disturbances, (2) their strength in the projected warmer climate, (3) the impact of offshore bathymetry on the propagation of meteotsunami waves and (4) the relative importance of the travelling meteotsunami waves generated along the Italian coasts versus the locally generated waves near the Croatian coasts. Moreover, these questions are also relevant to other meteotsunami hot-spots where they could provide critical information to assess both meteotsunami climate and coastal hazards.

To investigate these impacts, we test the sensitivity of meteotsunami generation and propagation by carrying out process-oriented numerical experiments in the Adriatic Sea (as described in Figure 1) for six historical meteotsunami events previously studied with the Adriatic Sea and Coast (AdriSC) atmosphere-ocean operational model (Denamiel et al., 2019a, 2019b). The events occurred on 25 and 26 June 2014, 28 June 2017, 1 July 2017, 31 March 2018 and 9 July 2019. The experiments consist of (1) evaluating the capacity of the AdriSC model to reproduce in re-analysis mode the historical events, in both the atmosphere and the ocean, (2) testing the impact of orography on the meteotsunami genesis, in the atmosphere only, by removing the Apennines mountains, (3) assessing the impact of far future extreme climate changes on the meteotsunami generation and propagation, in both the atmosphere and the ocean, and (4) analysing the impact of bathymetry and thus the Proudman resonance, in the ocean only, by flattening the deepest parts of the Adriatic Sea.

Our main findings are summarized in Figure 2, presenting the peaks in time of both meteotsunami wave and pressure disturbance extremes for each event over each subdomain (except for the Apennines sub-domain which does not cover the Adriatic Sea). They show that:

- meteotsunami-favourable conditions are likely to be largely increased within the Dalmatian Islands sub-domain in both atmosphere and ocean under a projected extreme warming climate (RCP 8.5 experiment). This is particularly relevant as the strongest and most destructive meteotsunami events occur within this sub-domain (Vilibić et al., 2016; Denamiel et al., 2018, 2020);

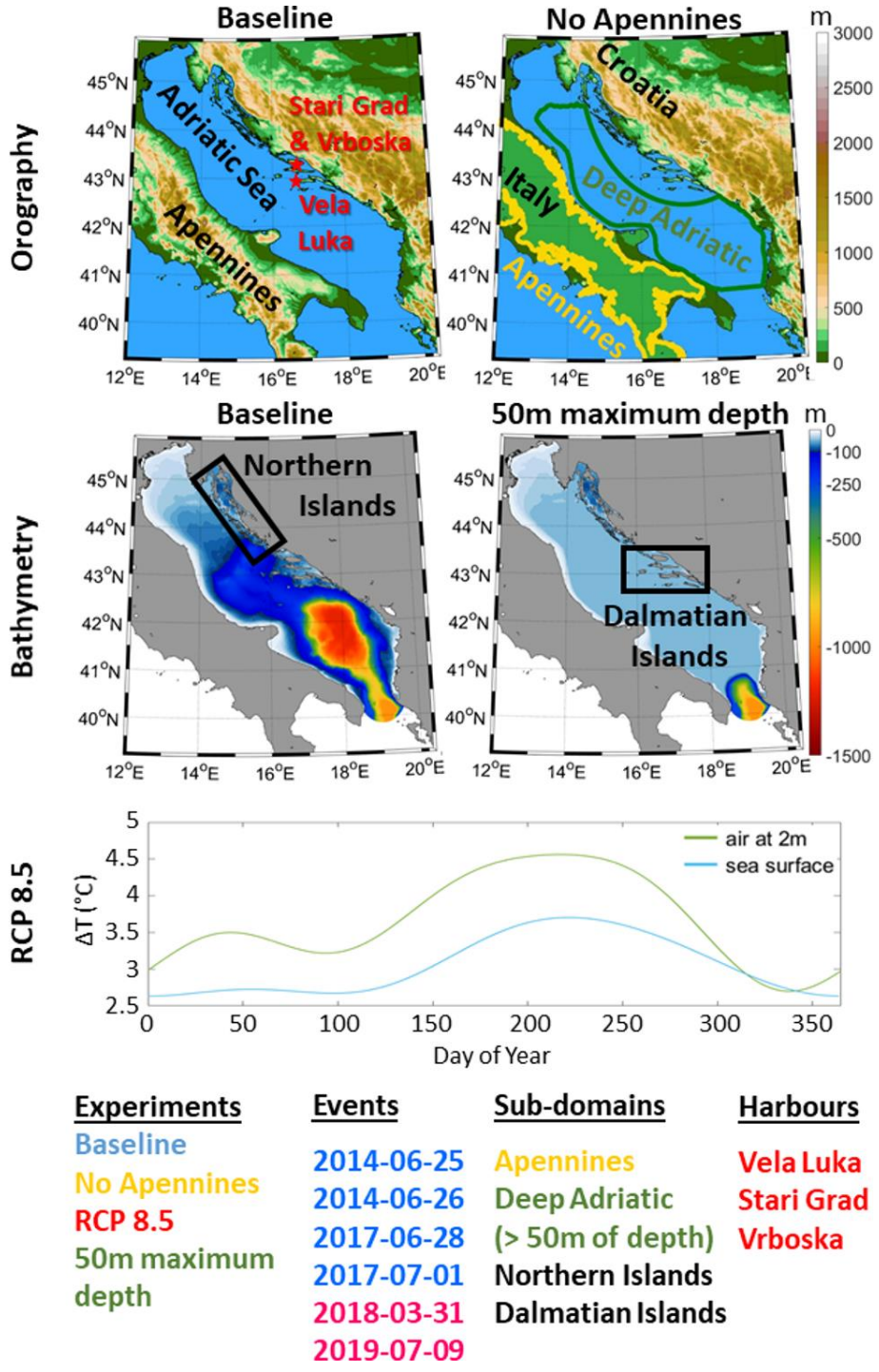

Figure 1. Experimental design of the study (after Denamiel et al., 2022a). *Orography of the atmospheric models (top panels), bathymetry of the ocean models (middle panels) and daily climatology of the temperature changes (ΔT) under climate scenario RCP 8.5 over the atmospheric and ocean domains (bottom panel) used for the four experiments (Baseline, No Apennines, RCP 8.5 and 50m maximum depth), the six studied meteotsunami events (i.e. four Calm Weather events: 25 and 26 June 2014, 27 June 2017, 1 July 2017 and two Stormy Weather events: 31March 2018 and 9 July 2019), the four chosen sub-domains (Apennines, Deep Adriatic, Northern Islands and Dalmatian Islands) and the three sensitive harbour locations (Vela Luka, Stari Grad and Vrboska).*

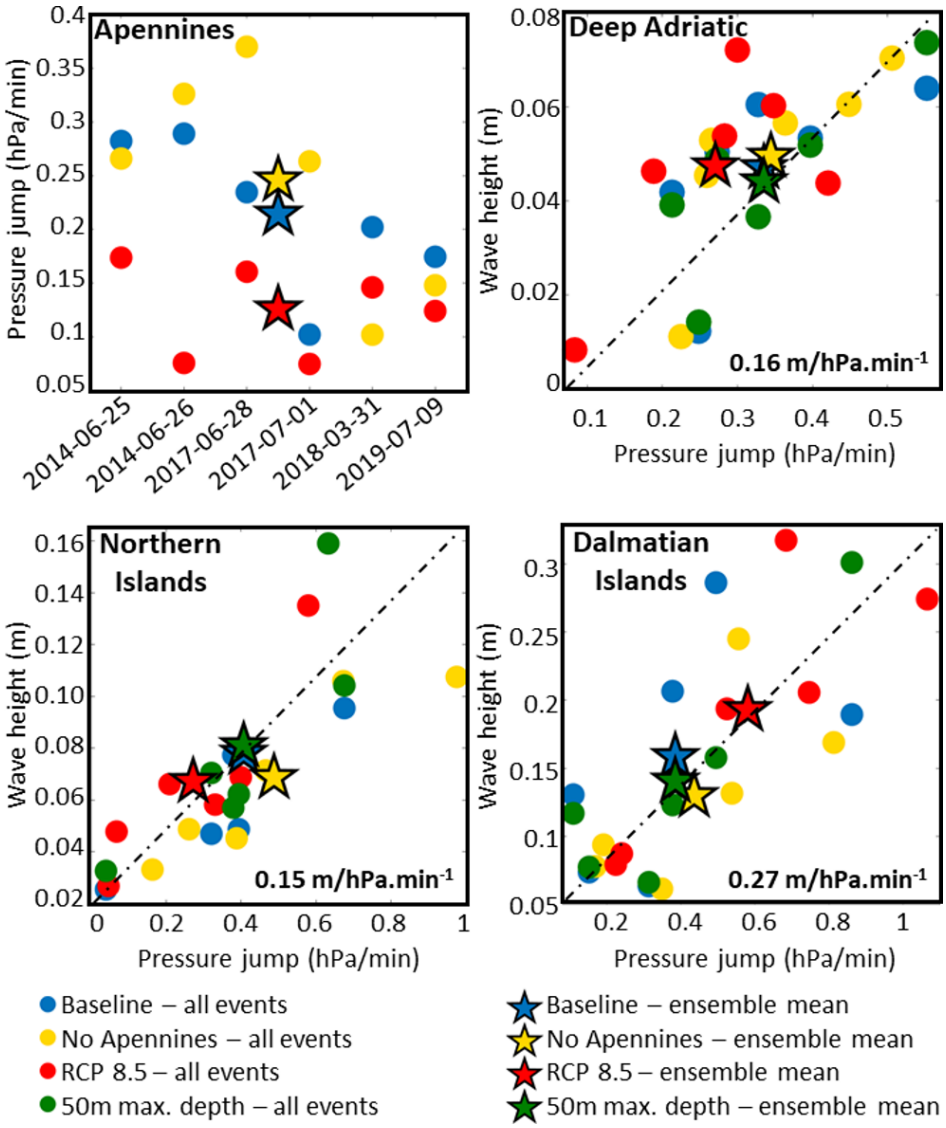

Figure 2. Summary of the findings (after Denamiel et al., 2022a). *For the Baseline, No Apennines and RCP 8.5 experiments, peak of the time variations of the 98th percentile for the mean sea-level pressure jump in the atmosphere depending on the six selected events for the Apennines sub-domain (top left panel). For the four different experiments and all the selected events, peak of the time variations of the 98th percentile for the filtered mean sea-level height (i.e. meteotsunami wave height in the ocean), depending on the peak of the time variations of the 98th percentile for the air-pressure rate of change in the atmosphere for the Deep Adriatic, Northern Islands and Dalmatian Islands sub-domains. For these sub-domains, the linear relationship between the atmospheric disturbance jump and the meteotsunami wave height is given as m/hPa for all events and experiments.*

- however, meteotsunami waves are projected to decrease in the adjacent Northern Islands subdomain under warmer climate (the RCP 8.5 experiment). Therefore, meteotsunami-favourable conditions are geographically limited due to, for example, the regional bathymetries (flat bathymetry off the Northern Islands sub-domain versus complex and changing bathymetry off the Dalmatian Islands sub-domain) or the location of the pressure disturbances during the studied events;
- flattening of the bathymetry (the 50m maximum depth experiment) substantially decreases the meteotsunami waves in the Dalmatian Islands sub-domain. This indicates that no Proudman resonance occurs within the Deep Adriatic sub-domain where the bathymetry is flat. In other

words, the speed of atmospheric disturbances is presumably not matching the speed of the long ocean waves in this sub-domain (i.e. 22 m/s). In addition, the flattening is found to divert the meteotsunami waves from the hot-spot locations to neighbouring coastal regions. Indeed, changing bathymetry may channelize the meteotsunami energy to certain locations (Sheremet et al., 2016; Šepić et al., 2018), similarly to tsunami propagation over ridges and channels (Titov et al., 2005);

- removing the Apennines (the No Apennine experiment) does not substantially change the intensity of the meteotsunamigenic disturbances (except an increase within the Apennines subdomain) but results in different spatial patterns, particularly for the Calm Weather situations. In the ocean, the resulting meteotsunami waves are slightly stronger, presumably due to different characteristic of the meteotsunamigenic disturbances (e.g. speed or propagation direction). Therefore, the meteotsunamigenic disturbances are not generated by the orography, just being modulated, while their origin is presumably driven by shear instabilities or similar processes that normally generate atmospheric internal gravity waves (Plougonven and Zhang, 2014). That may apply for other world locations vulnerable to meteotsunami events (e.g. the Balearic Islands) for which mountains are also suspected to have a substantial role in the meteotsunami genesis (Jansá and Ramis, 2021).

2. Mapping planetary meteotsunami hazard coming from volcano-generated Lamb waves

Catastrophic events such as volcano explosions (Choi et al., 2003) or asteroid impacts (Chapman and Morrison, 1994, Morgan et al., 2022) are known to cause extreme damages near their epicentres but also to affect the entire planet through megatsunamis (Kharif and Palinovsky, 2005), acidification of the atmosphere and ocean (Ohno et al., 2014), aerosol-driven reduction of solar radiation (Kring et al., 1996), and many other planetary-scale processes. However, the global impact of atmospheric waves (Matoza et al., 2022) generated during these events, including acoustic-gravity waves (Yeh and Liu, 1974) and the most prominent Lamb waves (Lamb, 1911; Bretherton, 1969), remains sporadically documented. Lamb waves propagate horizontally in the atmosphere with a speed close to the mean sound speed (Dragoni and Santoro, 2020) and can circle the globe multiple times (Press and Harkrider, 1966; Amores et al., 2022). They are associated with surface pressure oscillations of several hectopascals (hPa) per minute (Harrison, 2022) and their energy is dissipated towards the thermosphere (Forbes et al., 1999) via the ionosphere. In the worldwide oceans, they excite atmospheric tsunamis or meteotsunamis – long-waves in the tsunami frequency band generated by atmospheric disturbances (Pattiaratchi and Wijeratne, 2015; Rabinovich, 2020) – which spread with much greater speeds than tsunami waves generated by volcanic eruptions or seismic activity (Satake et al., 2020; Adam, 2022).

We carried out a 5-day long simulation of the Lamb wave-driven ocean waves generated by the Hunga eruption (Baseline simulation, hereafter) by coupling off-line the atmospheric model TIGAR (Vasylkevych and Žagar, 2021) (Transient Inertia-Gravity And Rossby wave dynamics model) with the global ocean model ATAL (Atmospheric Tsunamis Associated with Lamb waves). The TIGAR model solves the primitive equations in terrain-following coordinates using the Hough harmonics as the basis functions. In this representation, the Rossby and inertia–gravity waves are prognostic quantities, an approach especially suitable for studying gravity wave dynamics on the sphere. The model includes a realistic orography on the computational grid T170 that corresponds to the regular Gaussian grid of 680 and 320 grid points in the longitudinal and latitudinal directions, respectively. The ATAL model was specifically developed and implemented to reproduce the planetary meteotsunami waves generated by intense atmospheric forcing. It is based on the barotropic version (2DDI) of the Advanced CIRCulation (ADCIRC) unstructured model (Luettich et al., 1991) which solves the shallow-water equations in the ocean. The ATAL unstructured mesh used in this study was designed not only to properly capture the atmosphere-ocean interactions at the basin scale, but also to partially reproduce the coastal and nearshore meteotsunami transformation. It was produced with

the OceanMesh2D (Roberts et al., 2019) software for resolutions ranging from 20 km in the deep-ocean to 1.5 km along the worldwide coastlines using (1) the Global Self-consistent, Hierarchical, High-resolution Geography Database (GSHHG) fine resolution coastline (Wessel and Smith, 1996) and (2) the bathymetry from the GEBCO_2021 15 arc-second grid (GEBCO Compilation Group, 2021). The final mesh is composed of 6 864 084 nodes forming 13 306 437 triangular elements with a bathymetry ranging from a minimum of 1 m at the coast to 9823 m in the deepest part of the ocean.

A total of 12 different simulations are analysed in this study. First, the Baseline simulation (Figure 3A) is reproducing as realistically as possible the Lamb waves in the atmosphere (with speed of 318 m/s) and the meteotsunamis in the ocean for a 5-day long period after the Hunga eruption. Then, ten 2-day long process-oriented simulations are performed in order to find the speeds of the atmospheric waves leading to the maximum meteotsunami amplification under full Proudman resonance. For these simulations, the timeline of the Baseline atmospheric response is artificially rescaled by r = 1.25 (speed of 254 m/s), 1.40, 1.50, 1.60, 1.65, 1.75, 2.00, 3.00, 4.00 and 5.00 (speed of 64 m/s), thereby proportionally reducing the speed of the Lamb waves. The simulation leading to full Proudman resonance is referred to as simulation P. Finally, in the last 2-day long simulation (simulation A) used to assess the destructive potential of truly catastrophic events, the amplitude of the Lamb waves used in the Baseline simulation is multiplied by 10 before forcing the ocean model.

In the ocean, away from the shore, the meteotsunamis simulated by ATAL travel at a speed similar to the Lamb wave and have amplitudes of 1-3 cm in the deep-ocean and up to 5 cm near the source. As less than 1 % of the ocean depths are greater than 6000 m, the Froude number is almost always greater than 1.3 and not favourable to Proudman resonance for Lamb wave-driven meteotsunamis. Consequently, away from the shore, the planetary meteotsunami waves are not amplified by resonance and their amplitudes depend only on the intensity of the atmospheric forcing. However, nearshore wave transformations such as shoaling, reflection, refraction, and diffraction (Titov et al., 2005) are the main drivers of the meteotsunami surges along the coastlines. The cumulative density function (CDF; Figure 3B) shows that meteotsunami surges above 20 cm hit less than 1 % of the worldwide coastal areas.

Resulting CDF distributions of the meteotsunami surges (Figure 3B) show that the most extreme meteotsunami surges occur for scaling factors between 1.50 and 1.65, and thus for atmospheric waves with phase speeds between 193 m/s and 212 m/s. Under these conditions, 30 % of the worldwide coastlines are hit by meteotsunami surges higher than 35 cm (the 99.9th percentile value of the Baseline simulation). More importantly, the highest meteotsunami surges are obtained for r = 1.50 (212 m/s), which is consequently assumed to be the condition most favourable to Proudman resonance. Additionally, as the ocean depths strongly impact the resonance, the meteotsunami amplification is highly geographically dependent, even under full Proudman resonance (Figure 3C). It is particularly pronounced west of the northwest American coast where the maximum sea levels are 15 times greater than in the Baseline simulation. Somewhat weaker, but still a significant meteotsunami amplification (i.e., about 80 to 90 %), is obtained in the shallower oceans and seas (e.g., the Arctic Ocean and the Mediterranean Sea).

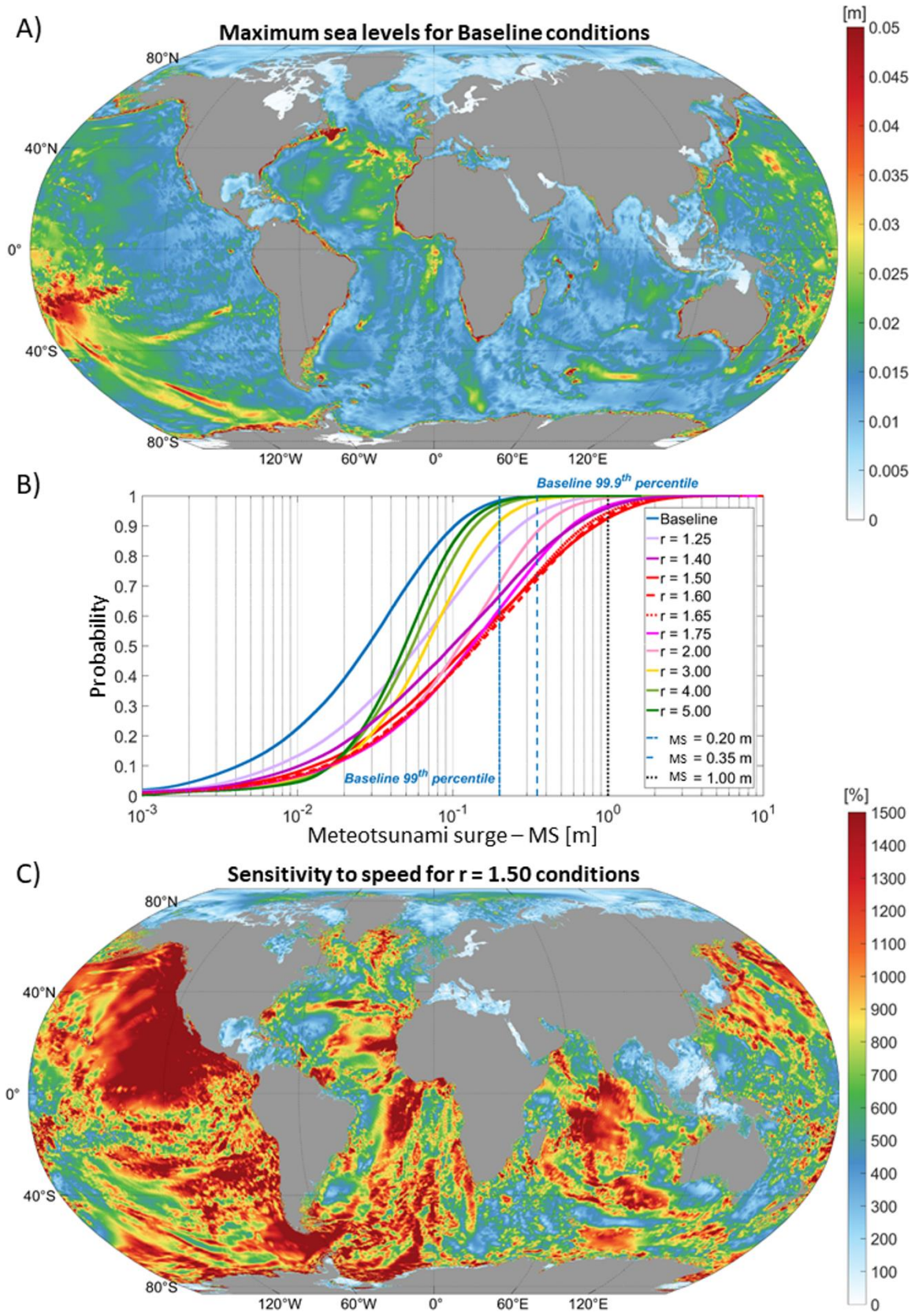

Figure 3. Distributions of the maximum sea levels after 48 hours of Hunga simulation (after Denamiel et al., 2022b). *(**A**) Baseline simulation (r = 1.00), (**B**) cumulative density functions of the meteotsunami surges (MS) for Baseline and sensitivity simulations with scaling factor r applied to the atmospheric wave phase speed varying between 1.25 and 5.00, and (**C**) sea level ratios between the r = 1.50 conditions and the Baseline simulation multiplied by 100 %. Scaling factor r = 1.50 generates the highest meteotsunami surges.*

3. Conclusions

In the last twelve months of this ECMWF Special Project, several research activities have been carried out to properly tackle different aspects of meteotsunami hazard. Investigations of future climate of meteotsunamis, by applying pseudo-global warming methodology for projecting climate change, is innovative and done for the very first time for this potentially destructive coastal hazard, Further, the role of mountains and bathymetry has been tested, reaching a conclusion that the mountains are not the generator but only the modulator of the meteotsunamigenic disturbances. The second study is – for the first time – providing global meteotsunami hazard from the waves generated by volcanic explosions, which are rare but potentially destructive events by all means. Thus, our research has a potential to be used for early warning systems, to which further hazards studies are needed and would be continued to research by numerical models on this ECMWF Special Project.

References

Adam, D., 2022. Tonga volcano eruption created puzzling ripples in Earth's atmosphere. *Nature* 601, 497. https://doi.org/10.1038/d41586-022-00127-1

Amores, A. et al., 2022. Numerical simulation of atmospheric Lamb waves generated by the 2022 Hunga-Tonga volcanic eruption. *Geophys. Res. Lett.* 49, e2022GL098240. https://doi.org/10.1029/2022GL098240

Bretherton, F., 1969. Lamb waves in a nearly isothermal atmosphere. *Q. J. Roy. Meteorol. Soc.* **95**, 754-757. https://doi.org/10.1002/qj.49709540608

Choi, B.H. et al., 2003. Simulation of the trans-oceanic tsunami propagation due to the 1883 Krakatau volcanic eruption. *Nat. Hazards Earth Syst. Sci.* 3, 321-332. https://doi.org/10.5194/nhess-3-321-2003

Chapman, C.R. & Morrison, D., 1994. Impacts on the Earth by asteroids and comets: assessing the hazard. *Nature* 367, 33-40. https://doi.org/10.1038/367033a0

Denamiel, C., Šepić, J., & Vilibić, I., 2018. Impact of geomorphological changes to harbor resonance during meteotsunamis: The Vela Luka Bay test case. *Pure Appl. Geophys.* 175, 3839–3859. https://doi.org/10.1007/s00024-018-1862-5

Denamiel, C., Šepić, J., Ivanković, D., & Vilibić, I., 2019a. The Adriatic Sea and Coast modelling suite: Evaluation of the meteotsunami forecast component. *Ocean Modell.* 135, 71–93. https://doi.org/10.1016/j.ocemod.2019.02.003

Denamiel, C., Šepić, J., Huan, X., Bolzer, C., & Vilibić, I., 2019b. Stochastic surrogate model for meteotsunami early warning system in the eastern Adriatic Sea. *J. Geophys. Res. Oceans* 124, 8485–8499. https://doi.org/10.1029/2019JC015574

Denamiel, C., Huan, X., Šepić, J., & Vilibić, I., 2020. Uncertainty propagation using polynomial chaos expansions for extreme sea level hazard assessment: The case of the eastern Adriatic meteotsunamis. *J. Phys. Oceanogr.* 50(4), 1005-1021. https://doi.org/10.1175/JPO-D-19-0147.1

Denamiel, C., Tojčić, I., Vilibić, I., 2022a. Meteotsunamis in orography-free, flat bathymetry and warming climate conditions. *Journal of Geophysical Research Oceans* 127, e2021JC017386. https://doi.org/10.1029/2021JC017386

Denamiel, C., Vasylkevych, S., Žagar, N., Zemunik, P., Vilibić, I., 2022b. Destructive potential of planetary meteotsunami waves beyond the Hunga volcano eruption (Tonga). Earth and Space Science Open Archive [preprint]. https://doi.org/10.1002/essoar.10511565.1

Dragoni, M. & Santoro, D., 2020. A model for the atmospheric shock wave produced by a strong volcanic explosion. *Geophys. J. Int.* 222, 735-742. https://doi.org/10.1093/gji/ggaa205

Forbes, J.M. et al., 1999. Lamb waves in the lower thermosphere: Observational evidence and global consequences. *J. Geophys. Res. Space Phys.* 104, 17107-17115. https://doi.org/10.1029/1999JA900044

GEBCO Compilation Group, 2021. GEBCO 2021 Grid [dataset]. https://doi.org/10.5285/c6612cbe-50b3-0cff-e053-6c86abc09f8f

Harrison, G., 2022. Pressure anomalies from the January 2022 Hunga Tonga–Hunga Ha'apai eruption. *Weather* 77, 87-90. https://doi.org/10.1002/wea.4170

Jansá, A., & Ramis, C., 2021. The Balearic rissaga: from pioneering research to present-day knowledge. *Nat. Hazards* 106, 1269-1297. https://doi.org/10.1007/s11069-020-04221-3

Kharif, C. & Pelinovsky, E., 2005. Asteroid impact tsunamis. *C. R. Phys.* 6, 361-366. https://doi.org/10.1016/j.crhy.2004.12.016

Kring, D.A., Melosh, H.J. & Hunten, D.M., 1996. Impact-induced perturbations of atmospheric sulfur. *Earth Planet. Sci. Lett.* 140, 201-212. https://doi.org/10.1016/0012-821X(96)00050-7

Lamb, H., 1911. On atmospheric oscillations. *Proc. R. Soc. London Ser. A* 84, 551–572. https://doi.org/10.1098/rspa.1911.0008

Luettich, R. A., Birkhahn, R. H. & Westerink, J. J., 1991. Application of ADCIRC-2DDI to Masonboro Inlet. A brief numerical modeling study. Contractors Report to the US Army Engineer Waterways Experiment Station: North Carolina.

Matoza, R. S. et al., 2022. Atmospheric waves and global seismoacoustic observations of the January 2022 Hunga eruption, Tonga. *Science*. https://doi.org/10.1126/science.abo7063

Morgan. J.V. et al., 2022. The Chicxulub impact and its environmental consequences. *Nat. Rev. Earth Environ.* https://doi.org/10.1038/s43017-022-00283-y

Ohno, S. et al., 2014. Production of sulphate-rich vapour during the Chicxulub impact and implications for ocean acidification. *Nature Geosci.* 7, 279–282. https://doi.org/10.1038/ngeo2095

Orlić, M., Belušić, D., Janeković, I., & Pasarić, M., 2010. Fresh evidence relating the great Adriatic surge of 21 June 1978 to mesoscale atmospheric forcing. *J. Geophys. Res. Oceans* 115, C06011. https://doi.org/10.1029/2009JC005777

Pattiaratchi, C.B. & Wijeratne, E.M.S., 2015. Are meteotsunamis an underrated hazard?. *Philos. Trans. R. Soc. A* 373, 20140377. https://doi.org/10.1098/rsta.2014.0377

Plougonven, R., & Zhang, F., 2014. Internal gravity waves from atmospheric jets and fronts. *Rev. Geophys*. 52, 33–76. https://doi.org/10.1002/2012RG000419

Press, F. & Harkrider, D., 1966. Air-sea waves from the explosion of Krakatoa. *Science* 154, 1325-1327. https://doi.org/10.1126/science.154.3754.1325

Rabinovich, A.B., 2020. Twenty-seven years of progress in the science of meteorological tsunamis following the 1992 Daytona Beach event. *Pure Appl. Geophys.* 177, 1193–1230. https://doi.org/10.1007/s00024-019-02349-3

Roberts, K. J., Pringle, W. J. & Westerink, J. J., 2019. OceanMesh2D 1.0: MATLAB-based software for two-dimensional unstructured mesh generation in coastal ocean modelling. *Geosci. Model Dev.* 12, 1847–1868. https://doi.org/10.5194/gmd-12-1847-2019

Satake, K. et al., 2020. History and features of trans-oceanic tsunamis and implications for paleo-tsunami studies. *Earth-Sci. Rev.* 202, 103112. https://doi.org/10.1016/j.earscirev.2020.103112

Šepić, J., Rabinovich, A.B., Sytov, V.N., 2018. Odessa tsunami of 27 June 2014: observations and numerical modelling. *Pure Appl. Geophys.* 175, 1545-1572. https://doi.org/10.1007/s00024-017-1729-1

Sheremet, A., Gravois, U., & Shrira, V., 2016. Observations of meteotsunami on the Louisiana shelf: a lone soliton with a soliton pack. *Nat. Hazards* 84, 471-492. https://doi.org/10.1007/s11069-016-2446-2

Titov, V., Rabinovich, A. B., Mofjeld, H. O., Thomson, R. E., & González, F. I., 2005. The global reach of the 26 December 2004 Sumatra Tsunami. *Science* 309, 2045-2048. https://doi.org/10.1126/science.1114576

Tojčić, I., Denamiel, C., & Vilibić, I., 2021. Performance of the Adriatic early warning system during the multi-meteotsunami event of 11–19 May 2020: an assessment using energy banners. *Nat. Hazards Earth Syst. Sci*. 21, 2427–2446. https://doi.org/10.5194/nhess-21-2427-2021

Vasylkevych, S. & Žagar, N., 2021. A high-accuracy global prognostic model for the simulation of Rossby and gravity wave dynamics. *Q. J. Roy. Meteorol. Soc.* 147, 1989-2007. https://doi.org/10.1002/qj.4006

Vilibić, I., Šepić, J., 2009. Destructive meteotsunamis along the eastern Adriatic coast: Overview. *Physics and Chemistry of the Earth* 34, 904-917. https://doi.org/10.1016/j.pce.2009.08.004

Vilibić, I., Šepić, J., Rabinovich, A. B., & Monserrat, S., 2016. Modern approaches in meteotsunami research and early warning. *Front. Mar. Sci*. 3, 57. https://doi.org/10. 3389/fmars.2016.00057

Vilibić, I., Denamiel, C., Zemunik, P., Denamiel, C., 2021. The Mediterranean and Black Sea meteotsunamis: An overview. *Natural Hazards* 106, 1223–1267. https://doi.org/10.1007/s11069-020-04306-z

Vučetić, T., Vilibić, I., Tinti, S., & Maramai, A., 2009. The Great Adriatic flood of 21 June 1978 revisited: An overview of the reports. *Phys. Chem. Earth* 34, 894–903.

Yeh, K. C. and C. H. Liu, 1974. Acoustic-gravity waves in the upper atmosphere. *Rev. Geophys.* 12, 193-216. https://doi.org/10.1029/RG012i002p00193

Wessel, P. & Smith, W. H. F., 1996. A global, self-consistent, hierarchical, high-resolution shoreline database. *J. Geophys. Res.* 101(B4), 8741–8743. https://doi.org/10.1029/96JB00104